Original Article
DOI: 10.4274/tjps.galenos.2021.48961

Preparation and Characterization of Chitosan and Inclusive Compound Layered Gold Nanocarrier to Improve the Antiproliferation Effect of Tamoxifen Citrate in Colorectal Adenocarcinoma (Caco-2) and Breast Cancer (MCF-7) Cells

Short title*:* Characterization of Gold Nanocarrier for Cancer Therapy

Yahia Kahlous[1], Vijayaraj Kumar Palanirajan[1*], Melbha Starlin[1], Jeetendra Singh Negi[1], Shiau-Chuen Cheah[2]
[1]Faculty of Pharmaceutical Sciences, UCSI University, no. 1, Jalan Menara Gading, Taman Connaught, Cheras 56000 Kuala Lumpur, Malaysia
[2]Faculty of Medicine & Health Sciences, UCSI University, no. 1, Jalan Menara Gading, Taman Connaught, Cheras 56000 Kuala Lumpur, Malaysia

Corresponding Author Information
Vijayaraj Kumar Palanirajan
vijayarajkumar_p@yahoo.com
+60103782399
https://orcid.org/0000-0003-1129-7084
19.05.2021
17.09.2021
15.10.2021

UNCORRECTED PROOF

ABSTRACT
Introduction: Cancer diseases has been linked to huge number of causes that leads to the death in this century, along with cardiovascular diseases and lung diseases. Most death-leading types of cancer are colon cancer, lung cancer, breast cancer, and prostate cancer. Due to the remarkable properties of gold nanocarrier, they are used to deliver and improve tamoxifen citrate activity on Caco-2 and MCF-7 cells.
Materials and Methods: In this study, preparation of gold nanoparticles, the zeta-potential and size, high resolution transient electron microscopy, HPLC, UV-vis spectra, fluorescence microscopy, Fourier infrared spectroscopy, and real-time cellular analysis xCELLigence technology were investigated.
Results: The zeta-average size of the Tam-β-CD-HA-Chi-Au nanocomposite is 82.02 nm with negative zeta potential of -23.6. Furthermore, HRTEM images showed that, successful formulation of polymer shell around Au core and the Au NPs shape is mostly spherical, triangle and irregular. Furthermore, the fluorescence microscope image showed proper cellular uptake of the Tam- β-CD-HA-Chi-Au nanocomposite in MCF-7 and Caco-2 cells. In addition, The Tam-β-CD-HA-Chi-Au nanocomposite significantly improved the cytotoxic activity of tamoxifen citrate on Caco-2 cells. The IC_{50} value of Tam was reduced from 8.55 µM to 5.32 µM after 48 hours of incubation time (p-value < 0.00001).
Conclusion: This research study showed that Tam-β-CD-HA-Chi-Au nanocomposite is a potential nanocarrier to deliver drug to Caco-2 and MCF-7 cancer cells, since it has improved the tamoxifen citrate activity on colorectal cancer cells. After all, the developed formula showed more effect on Caco-2 than MCF-7. The prepared nanocomposite could be used to improve the cancer therapy in clinical trials.

Keywords: Chitosan Gold Nanoparticles, Tamoxifen citrate and β-Cyclodextrin, MCF-7 cell line and Caco-2 cell line, Cytotoxicity and Cellular Uptake, Xcelligence RTCA Systems.

INTRODUCTION

Cancer diseases has been linked to huge number of causes that leads to the death in this era, along with cardiovascular diseases and lung diseases.[1] In general, cancer has widely spread in last few years, the number of cancer patients in America alone reaches, around 1,806,590 patients.[2] Most death-leading types of cancer are colon cancer, lung cancer, breast cancer, and prostate cancer. Among various cancer types, colorectal cancer has a high prevalence in the United States with 147,950 new patients and 53,200 expected deaths. Approximately 104,610 patients were identified with colon cancer and 43,340 were identified with rectal cancer during 2020.[3] The potential causes of colon cancer may be sporadic, hereditary or caused by the development of ulcerative colitis and Crohn's disease.[4]

Tamoxifen citrate (Tam) is most frequently used for the treatment of breast cancer by preventing the estrogen hormone from binding to its receptors.[5] The therapeutic dose of the tamoxifen was 10 mg to 40mg/day. The 15.2 mg tamoxifen citrate is equivalent to 10 mg of tamoxifen. Tumours are generally associated with irregular blood vessels with the ability for increasing permeation and poor lymphatic drainage that contribute to the retention inside tumours.[6] This improved permeability and retention (EPR) effect could be utilized by nanoparticles (NPs) to localize inside solid tumours.[7] Various nanocarriers formulations have been developed to improve chemotherapy.[8] Doxil and Myocet (doxorubicin liposomes) were the first class therapeutics to be approved for cancer therapy.[9] Other promising nanocarriers either approved or in clinical trials are nab-paclitaxel (albumin NPs)[10], SMANCS, CRLX-101 (campthothecin NPs) and NK-105 (paclitaxel micelle).[11] Moreover, nanocarriers could be decorated with targeting ligands for specific receptor on the tumour cells to improve cellular uptake.[12] Few nanocarriers for targeted drug delivery are also in clinical trials such as MM302 (HER-2 targeting), MBP-426 (TfR-targeting) and BIND-014 (PSMA-targeting).[13] In addition to therapeutic benefits, nanocarriers could also be used in cancer diagnosis. Inorganic NPs and particularly gold (Au) NPs have been used extensively to improve diagnosis of cancer tissue.[14]

One of the issues to be addressed with current chemotherapy is the ineffectiveness against multidrug resistant cancer cells.[15] Specifically, resilience against structurally and systematically unrelated drugs, is the primary concern in cancer treatment.[1] Cancer cells acquired resistance mainly due to the overexpression of drug efflux proteins, DNA repair activation and apoptotic signalling modification.[16] High interstitial fluid pressure of tumour stroma also hinders drug penetration which results into the development of drug resistance due to less drug exposure.[17] Furthermore, multidrug resistant cancer cells strongly reduces internalization of drug across the cell membrane with the help of P-glycoprotein (P-Gp) efflux pumps.[18] Recently, scientists started to utilize several unique characteristics of extracellular tumor microenvironment like acidic extracellular pH, specific enzymes and hypoxia condition. The interest in chitosan (Chi) is derived from chitin by deacetylation process to several degrees. The polymer is considered as chitosan when the degree of acetylation is less than 50%, which is soluble in acidic solutions.[19] Moreover, Chi has increased for its cationic nature and mucoadhesive properties which improve drug absorption.[20] Chi NPs not only have the ability to deliver hydrophilic and hydrophobic molecules but also stabilize pharmaceutical ingredients against enzymatic degradation and therefore thus improve the bioavailability and prolong the drug action.[21] The present study is an attempt to develop a NPs drug delivery system using β-cyclodextrin (β-CD)-based inclusion complexes to enhance the cellular uptake of nanocarriers and increase the internalization of Tam inside the cancer cells and improve its efficacy.

UNCORRECTED PROOF

MATERIALS AND METHODS

Materials

Gold (III) chloride 99% (Sigma-Aldrich, USA), chitosan low molecular weight (Sigma-Aldrich,USA), β-cyclodextrin >97% (Sigma-Aldrich, USA), Sodum citrate tribasic dihydrate (Sigma-Aldrich, USA), Hyaluronic acid sodium salt (Sigma-Aldrich, USA), Tamoxifen citrate (Sigma-Aldrich, USA), Sodium tripolyphosphate (TPP) 85% (Sigma-Aldrich, USA), Dulbecco's Modified Eagle's Medium (DMEM) (ATCC, USA), phosphate buffered saline (ATCC, USA), Trypsin-EDTA Solution (ATCC, USA), Penicillin-Streptomycin Solution (ATCC, USA), Fetal bovine serum (ATCC, USA), Trypsin-EDTA Solution (ATCC, USA), Caco-2 (ATCC HTB-37, USA) and MCF-7 (ATCC HTB22™, USA) cell lines.

Preparation of tamoxifen:β-Cyclodextrin (Tam:β-CD) inclusion compound

The Tam:β-CD inclusion compound was prepared in a 1:1 M ratio. Briefly, 10 mg of Tam and 10 mg of β-CD were completely dissolved in (2:1 v/v) the mixture of methanol and 30% of ammonium hydroxide. The solution was filtered through a 0.45 μ membrane filter, and the filtrate was evaporated under reduced pressure and dried in a vacuum oven (80 °C and 695 ± 69 mbar) (Figure 1A).[22, 23]

Preparation of Gold Nanoparticles

In brief, 2.5 mL of chloroauric acid ($HAuCL_4$) solution (1 $mg.ml^{-1}$) was mixed with 20 mL ultrapure water and the solution temperature was maintained at 80°C under magnetic stirring at 350 rpm. Then, Au NPs were formed by adding 1 mL of sodium citrate tribasic dihydrate solution (7 $mg.ml^{-1}$) and the stirring was continued until the colour of the solution changed to purple.

Preparation of Chitosan-Gold Nanoparticles

Chi-Au NPs were prepared by adding 0.2 mL Chi solution (0.5 $mg.ml^{-1}$) and 2.5 mL of $HAuCL_4$ solution (1 $mg.ml^{-1}$) along with 19.8 mL of ultrapure water at 80°C and 700 rpm. Then, 1 mL of sodium citrate tribasic dihydrate solution (7.5 $mg.ml^{-1}$) was added to the obtained solution and the stirring was continued until the colour of the solution changed to dark blue.

Preparation of Tam-β-CD-HA-Chi-Au nanocomposite

Briefly, 12.5 mL of $HAuCL_4$ solution (1 $mg.ml^{-1}$) was mixed with 1 mL Chi solution (0.5 $mg.ml^{-1}$) and 97.5 mL of ultrapure water was added under stirring at 500 rpm and temperature of 65°C for 30 minutes. Then, 2.5 mL of Tam-β-CD inclusion compound and 500 μg of hyaluronic acid (HA) were added to the solution. Finally, the formation of NPs was achieved by adding 3.66 mL of sodium citrate tribasic dihydrate solution (15 $mg.ml^{-1}$) along with 1.84 mL of TPP solution (1 $mg.ml^{-1}$) to the obtained solution under continuous stirring. The resulted NPs were centrifuged at 13000 rpm, dried by vacuum oven (80°C and 695 ± 69 mbar) and used for further studies.

Determination of Particle Size, Zeta-Potential and Polydispersity Index

Zeta-potential of Tam-β-CD-HA-Chi-Au nanocomposite was measured by doppler anemometry using zeta-sizer (Malvern instrument, Malvern, UK) at 25°C. Around 2 ml of samples were filtered by 0.20 μm syringe filtered and then filed in the zeta cell for measuring the size and charge of the nanocomposite.

High resolution Transient Absorption Microscopy (HRTEM)

High resolution transient absorption microscopy was conducted using JEM-2100F microscope. The structure and morphology of Tam-β-CD-HA-Chi-Au nanocomposite were determined. The sample was sonicated for 15 minutes. Then, one drop of the sample was placed on HRTEM grid and kept at room temperature of DAPI until it was completely dry. Thereafter, the morphology of the nanocomposite was observed, and high-quality images were taken.

UNCORRECTED PROOF

UV-visible Spectra

Optical properties of Au NPs solution were determined using double beam spectrophotometer, by scanning the spectra from 200 to 800 nm. Sodium citrate tribasic dihydrate and TPP solution were used as blank and ultrapure water was used as solvent. Au NPs, Chi-Au NPs and Tam-β-CD-HA-Chi-Au nanocomposite solutions were characterized as well.

Fourier transform infrared spectroscopy (FTIR) spectrometers

All spectra of samples were taken by the Thermo Fisher Scientific Nicolet iS5 spectrophotometer (Wiscon-sin, USA), utilizing OMNIC Software from 1000 to 4000 cm^{-1} at a data acquisition rate of 2 cm^{-1} per point.

Determination of Encapsulation and loading Efficiency.

To assess the encapsulation and loading efficiency (EE) of Au NPs, 5 mg of Tam-loaded Au NPs were dissolved in methanol, then filtered and centrifuged for 30 minutes at 13,000 rpm.[24, 25] The amount of Tam in supernatant was determined by HPLC and the EE was calculated using the following equation.[26] :

$$\mathrm{EE}(\%) = \frac{\text{total Tamoxifen citrate content} - \text{free Tamoxifen citrate content}}{\text{total Tamoxifen citrate content}} \times 100 \qquad \text{Eq.1}$$

Chromatographic Conditions

The HPLC system used for this study was Waters 2487 Dual λ Absorbance Detector equipped with Water 1515 Isocratic HPLC Pump and Supelco® Analytical column with 15 cm x 4.6 mm i.d.; 5 µm particle size. The mobile phase for gradient elution was composed by a solution of acetic acid and 1% of ammonium acetate in methanol (1:99) at flow was 1.5 $ml.min^{-1}$.[27] The 10 µL of the sample was injected into chromatographic system.

Cell Culture

MCF-7 (ATCC HTB22™) and Caco-2 (ATCC HTB-37) cells were routinely kept in DMEM containing 1% penicillin-streptomycin at 37°C and 10% fetal bovine serum in 5% CO_2 and 95% air.

Dynamic Assessment of Cytotoxic Effect of Tam-β-CD-HA-Chi-Au nanocomposites on Caco-2 and MCF-7 Cells using real-time cell analysis.

In this study, real-time cellular analysis xCELLigence (RTCA) technology was chosen for screening the cytopathic effect of nanocomposite by monitoring the cellular impedance of the cells in real-time during the complete time course of the experiment.[24] Background measurements were taken from the wells by adding 50 µL of DMEM media to E-plates 16. Then, MCF-7 and Caco-2 cells were seeded and plated at a density of $1x10^4$ cells/well in fresh DMEM media, grown overnight at 37℃ and 5% CO_2 to reach the log phase, then incubated with Tam, Tam-β-CD-Au NPs, and Tam-β-CD-HA-Chi-Au nanocomposite (each complex contained 23.69, 35.69, and 47.55 µM of Tam) or medium alone, and cell responses were monitored by taking RTCA DP instrument (ACEA Biosciences Inc., USA) readings every single 5 minutes for 24 hours and every 30 minutes for 48 hours. The kinetic profile of the cellular responses, the reduction in cell index, and IC_{50} values as per each complex were taken accordingly against their respective concentrations.[25]

Preparation of Rhodamine 6G-Labeled Tam-β-CD-HA-Chi-Au nanocomposite

The Vacuum-dried Tam-β-CD-HA-Chi-Au nanocomposite was redispersed in 5 mL DMSO solution followed by the addition of rhodamine 6G and 0.5 mL of NaOH (0.1 M) was dissolved in methanol at 10.0 $mg.ml^{-1}$concentration. The nanocomposites were incubated with rhodamine 6G solution for 24 hours in the dark at environmental temperature. The prepared rhodamine-labelled Tam-β-CD-HA-Chi-Au nanocomposites were collected by centrifugation and washed 3 times with methanol until the free rhodamine 6G could not be seen in the

UNCORRECTED PROOF

supernatant. Then, Tam-β-CD-HA-Chi-Au nanocomposites were resuspended in 5 mL phosphate buffered saline (PBS) after centrifugation.

Cellular uptake Assessment of Tam-β-CD-HA-Chi-Au nanocomposites by Fluorescence Microscopy

A Zeiss Axio Vert.A1 inverted microscope (Carl Zeiss, Germany) outfitted with HBO 50 W mercury vapour lamp and exciter/emitter filter combinations were used. Filter 38 (495 nm excitation and 517 nm emission) was used to observe FITC stained cellular membrane with green colour. Filter 43 (550 nm excitation and 573 nm emission) was used to observe rhodamine-labelled Tam-β-CD-HA-Chi-Au nanocomposites with red colour and filter 49 (359 nm excitation and 457 nm emission) was used to observe 4′,6-diamidino-2-phenylindole (DAPI) stained cells with blue colour. MCF-7 and Caco-2 cells were seeded at density of $1x10^5$ cells/well. Then, the cells were shifted to centrifuge tubes containing serum free medium supplemented with rhodamine-labelled Tam-β-CD-HA-Chi-Au nanocomposites (100 $\mu g.ml^{-1}$) and kept in dark place for 6 hours. Instantly after 6 hours, the cells were washed several times with phosphate buffered saline and fixed by 100 µL of 37% formaldehyde then left at environmental temperature for 10 minutes followed by additional washing steps. The cells were centrifuged at 4000 rpm and the supernatant was discarded. Then, 10 µL of DAPI stain (1 $\mu g.ml^{-1}$) and 10 µL of FITC stain (60 $\mu g.ml^{-1}$) were added. The cells were kept in the dark place for 20 minutes. Finally, the cells were centrifuged and separated, then resuspended in 20 µL of PBS and 1 µL of cell suspension was placed onto a glass slide, then the slide was coated with a coverslip.[28] The images of the cells were captured, under standardized setting and contact time, by fluorescent microscope and Zen 2010 software (Blue Edition) was utilized for image analysis.

RESULTS AND DISCUSSION

Preparation of Tam-β-CD-HA-Chi-Au Nanocomposite

Tam-β-CD-HA-Chi-Au nanocomposites were prepared as described by Turkevich *et al*.[29], with modification. Chitosan was used to offer sufficient surface area for loading the drug and improve drug delivery, hence it is chosen to be mixed with Au (III) chloride.[30] Then, ultrapure water was added under stirring at 500 rpm and at the temperature of 65°C for 30 minutes, followed by the adding of Tam-β-CD inclusion compound to improve Tam solubility. HA was added to enhance tumour permeability and NPs retention[31, 32] along with TPP solution which was used as cross-linker to form electrostatic attraction between positive charge Chi and negative charge TPP.[33] Finally, due to reduction properties of sodium citrate tribasic dihydrate, it was added to sodium citrate tribasic dihydrate to achieve the formation of Au NPs (Figure 1B) and it resulted on the repositioning and rigidization of both inclusion compound and Chi on the superficial of Au NPs to form Tam-β-CD-HA-Chi-Au nanocomposite.[29, 34]

UNCORRECTED PROOF

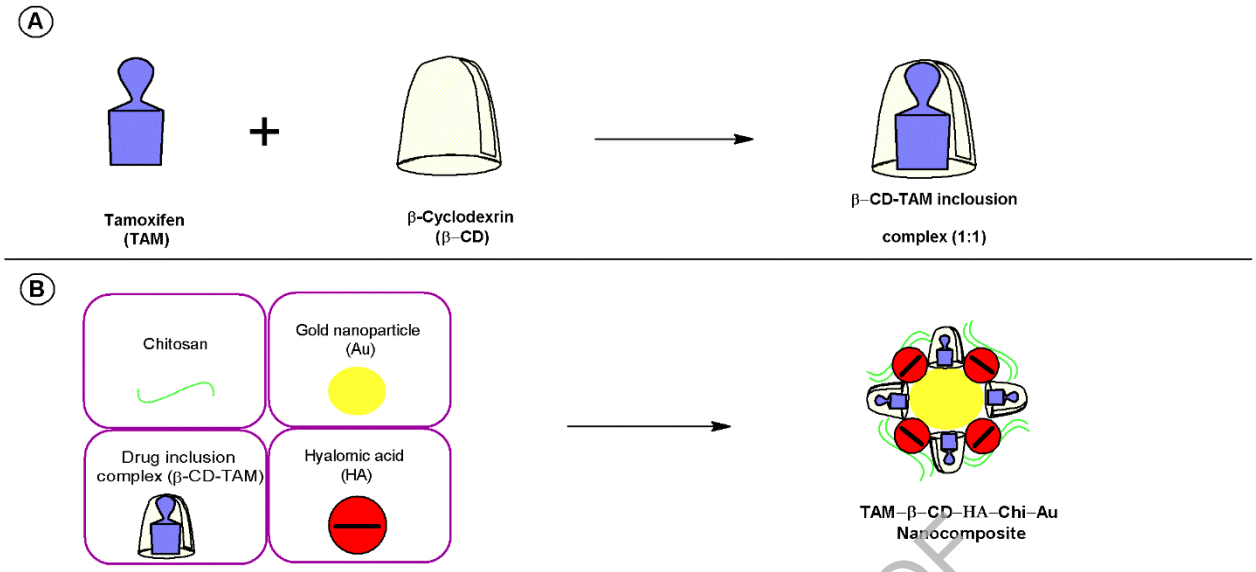

Figure 1 Schematic diagram describes the preparation steps of both β-CD-Tam inclusion complex (A) and Tam-β-CD-HA-Chi-Au nanocomposite (B).

Particle Size, Zeta Potential, and Polydispersity Index (PDI) Determination

The average size of the prepared NPs was 12.31 nm with -46.4 mV zeta potential for Au NPs, 21.66 nm with -37.7 mV zeta potential for Chi-Au NPs and 82.02 nm with -32.6 mV zeta potential and PDI 0.107 (Figures 2A and 2B) for Tam-β-CD-HA-Chi-Au nanocomposite (Table 1). Setyawati *et al.*[35], stated that the size of their Au NPs was 11 nm. Moreover, Regiel-Futyra *et al.*[36], reported that the size of Chi-Au nanoparticle was 26 nm which is similar to our average size of Chi-Au NPs. However, Kang *et al.*[37], prepared docetaxel cationic lipid-coated Au nanoparticle with a size of about 70 nm which is smaller than the size of our Tam-β-CD-HA-Chi-Au nanocomposite.

UNCORRECTED PROOF

Parameters	Au NPs	Chi-Au NPs	Tam-β-CD-HA-Chi-Au nanocomposite
Mean Particle Size	12.31	21.66	82.02
Zeta Potential	-46.4	-37.7	-32.6
PDI	0.544	0.557	0.107

Table 1. Mean particle size, zeta potential, and polydispersity index of the prepared gold nanoparticle.

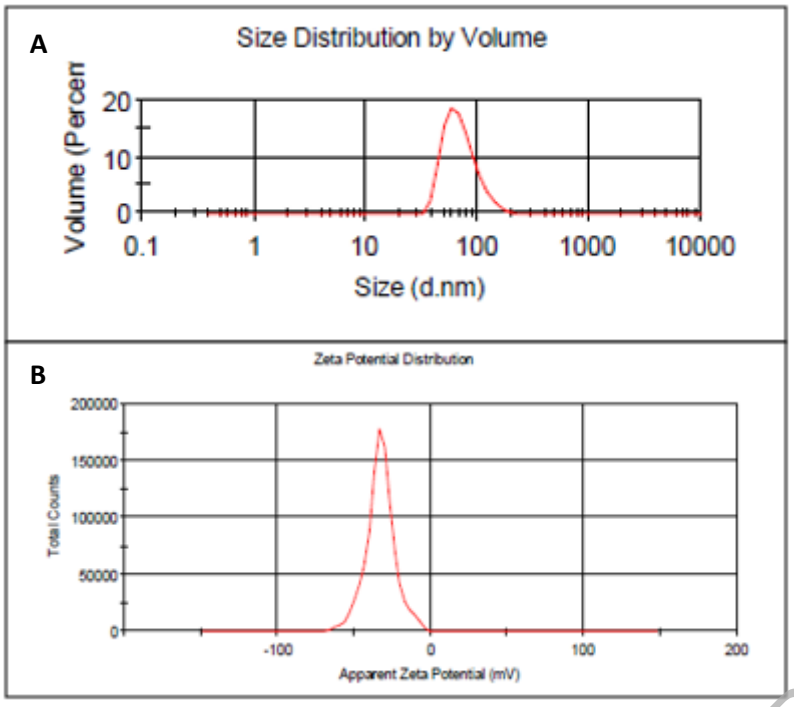

Figure 2. Size distribution of Tam-β-CD-HA-Chi-Au nanocomposite by volume (A), Zeta potential distribution of Tam-β-CD-HA-Chi-Au nanocomposite (B).

High Resolution Transmission Electron Microscope Studies

HRTEM images revealed that the Au occupied a central position, and a layer of polymers was surrounding the Au nanoparticles which indicate a successful formulation of Au NPs and a layer of Chi and inclusion complex was deposited on the surface of NPs (Figure 3C). Figure 3A-B presents different Au NPs shapes including spherical, hexagonal and irregular shapes. Regiel-Futyra *et al*,[36] reported that most of their Au NPs were in spherical shape. However, a previous research reported the presence of irregular NPs with average size of 33 nm.[38]

UNCORRECTED PROOF

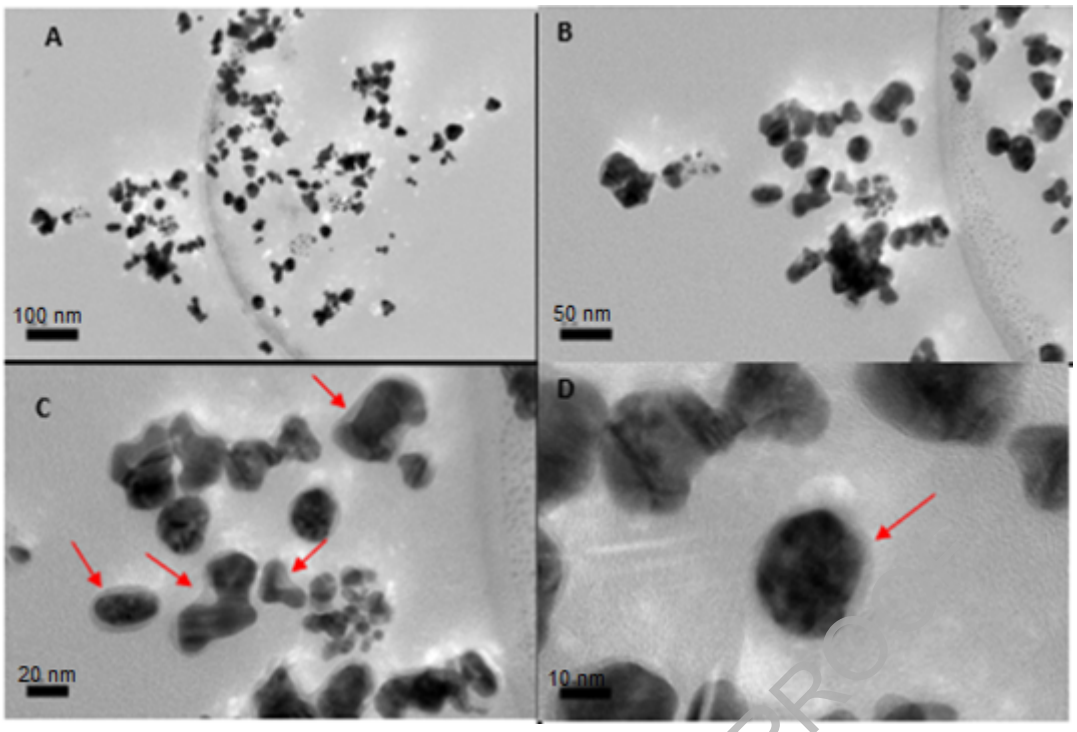

Figure 3. images of Tam-β-CD-HA-Chi-Au Nanocomposite. A and B show different Au NPs shapes including spherical, hexagonal and irregular. C and D show a successful formation of Chi and inclusion complex layer that surrounding Au NPs.

UV-vis Spectra

The reduction of chloroauric acid to Au NPs was confirmed by UV spectroscopy, by scanning the spectra from 200 to 800 nm (Figure 4D). The UV-vis spectra of GNPs revealed maximum absorbance at 233 and 529 nm, which indicated that the chloroauric acid was converted to Au NPs. Whereas, when Chi was incorporated with GNPs, the result showed a shifting in λ_{max} from 233 to 243 and from 529 to 527 nm. Noticeably, this shifting in λ_{max} resulted in changed of colour form purple (GNPs) to light violet colour (Chi-GNPs) (Figure 4A and 4B). However, the maximum absorbance of Tam-β-CD-HA-Chi-Au Nanocomposite was at 221 and 527 nm with dark violet colour (Figure 4C) (Table 2).

UNCORRECTED PROOF

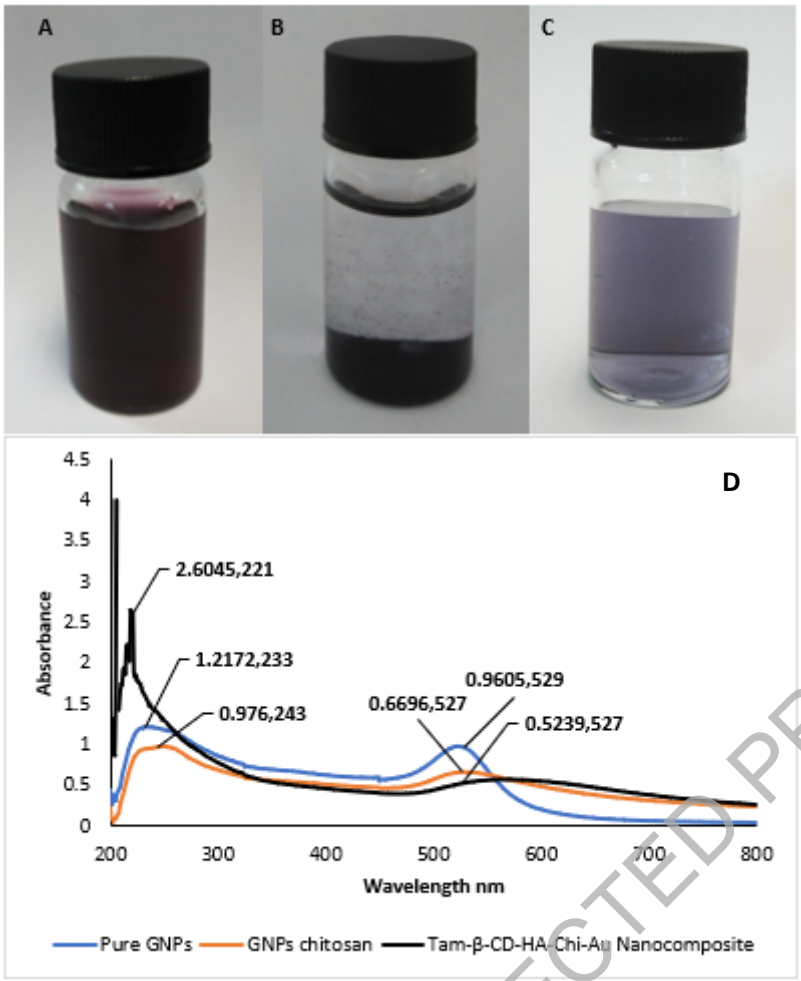

Figure 3. GNPs (A), Chi-GNPs (B), Tam-β-CD-HA-Chi-Au Nanocomposite (C), Absorption spectra of GNPs. The results demonstrated the correlation between the shifting in λmax and the formation of NPs (D).

UNCORRECTED PROOF

Nanoparticles	Absorbance(nm)
GNPs	233 and 529
Chi-GNPs	243 and 527
Tam-β-CD-HA-Chi-Au Nanocomposite	221 and 527

Table 2. The shifting in λ_{max} between GNPs, Chi-GNPs, and Tam-β-CD-HA-Chi-Au due to change in the chemical composition in nanocomposite is shown in the figure 3.

Determination of Encapsulation Efficiency

As previously described, the encapsulation efficiency (EE) of Au NPs can be calculated using equation (1) which was found to be 94.97%.

FTIR Characterization

A comparison was made of several FTIR spectra of analyzed samples to confirm the complex formation between Au NPs, Chi-Au NPs, inclusive compound, and Tam-β-CD-HA-Chi-Au nanocomposite. Figure 5B revealed that the characteristic peak of Chi at 1645 cm^{-1} disappeared and two new peaks appeared at 1623 cm^{-1} and 1567 cm^{-1}, respectively. This disappearance of the peaks can be explained by the attribution of the band to the linkage of the

phosphoric and ammonium ions. This new band at 1623 cm^{-1} was due to N-H vibrations in NH^{3+} ion. This showed the occurrence of the cross-linking between Chi and TPP and confirmed the formation of the polyelectrolyte complex. On the other hand, the characteristic peaks of Tam in the inclusion complex entirely vanished showing characteristic peaks at 1393 cm^{-1} (coupled in plane bending of CH_2), 2964 cm^{-1} (asymmetric stretching from CH_2), and at 3260 cm^{-1} (asymmetric and symmetric stretching of OH), Figure 5C indicated that Tam molecule was entirely inserted into the β-CD cavity. In Figure 5D, none of the characteristic peaks of Tam nor β-CD were observed as the inclusive compound was loaded into the NPs, but only the characteristic peaks of Chi and Au NPs were observed with slight shifting due to the surface interaction between Chi and Au NPs.

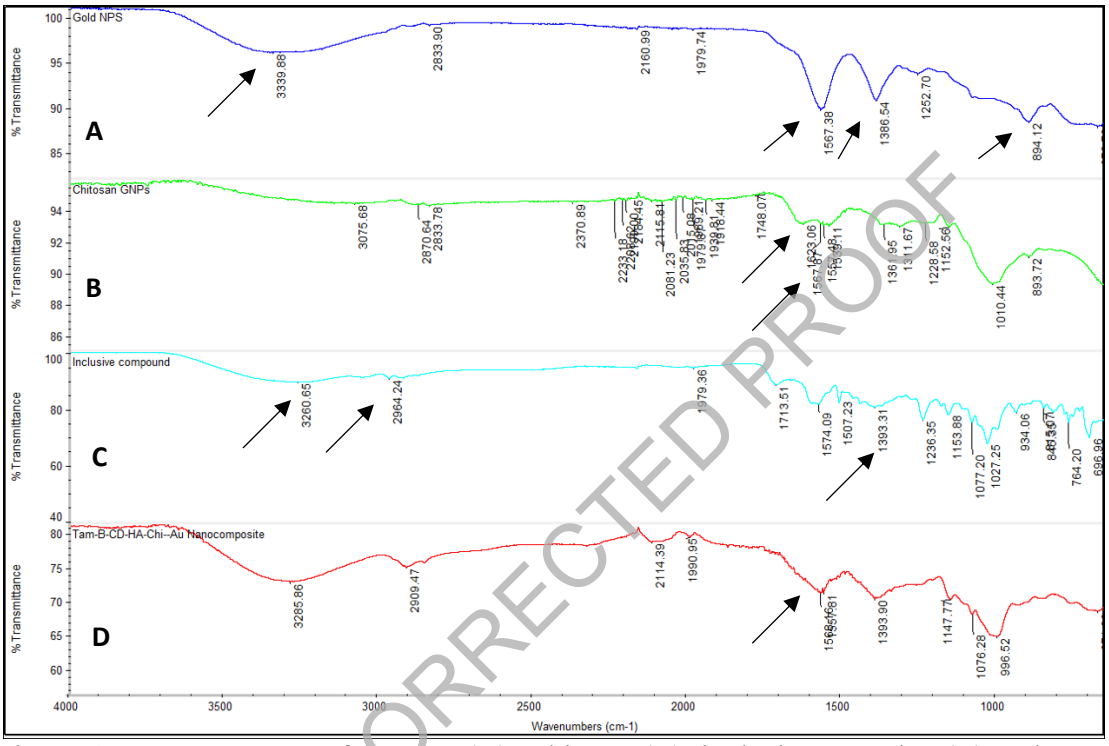

Figure 4. FTIR spectrum of Au NPs (A), Chi NPs (B), inclusion complex (C) and Tam-β-CD-HA-Chi-Au nanocomposite (D).

UNCORRECTED PROOF

Cellular Uptake of Tam-β-CD-HA-Chi-Au Nanocomposite Using Fluorescence Microscopy Techniques

The objective of fluorescence microscope imaging was to confirm the cellular uptake of NPs by Caco-2 and MCF-7 cells. As shown in Figure 6A, rhodamine stained the nanoparticles with a red colour and 4′,6-diamidino-2-phenylindole (DAPI) stained the nucleus with a blue colour, whereas fluorescein isothiocyanate (FTIC) stained cellular membrane with a green colour. According to the data presented in Figure 6A, Caco-2 cellular uptake of Tam-β-CD-HA-Chi-Au nanocomposite is time-dependent. The fluorescence microscopy indicated that the Tam-β-CD-HA-Chi-Au nanocomposite entered the cancer cell and localized near the nucleus. In other words, there was a portion of the Tam: β-CD-HA-Chi-Au nanocomposite was taken up by the cell and got localized next to the nucleus. In addition, fluorescence images showed a punctuated staining pattern due to intracellular aggregates of nanocomposites.

Hence, cellular uptake of the prepared Tam-β-CD-HA-Chi-Au nanocomposite was efficiently improved by Chi properties such as mucoadhesive and absorption enhancement. Moreover, the cellular uptake was also quantified by measuring the red light (due to rhodamine-labelled NPs) intensity per cell and as shown in Figures 6B,6C and 6D (Table 3). The observations suggested that the light intensity is directly correlated to the incubation time, therefore indicating that the developed formulation improved the cellular uptake of NPs in time-dependent manner. On the other hand, as shown in Figure 7, the Tam-β-CD-HA-Chi-Au nanocomposites did not appear at zero hour, indicating that absorption did not take place. However, at 1 h and 2 h, MCF-7 cellular uptake of Tam-β-CD-HA-Chi-Au nanocomposite was time-dependent with slight improvement in cellular uptake.

UNCORRECTED PROOF

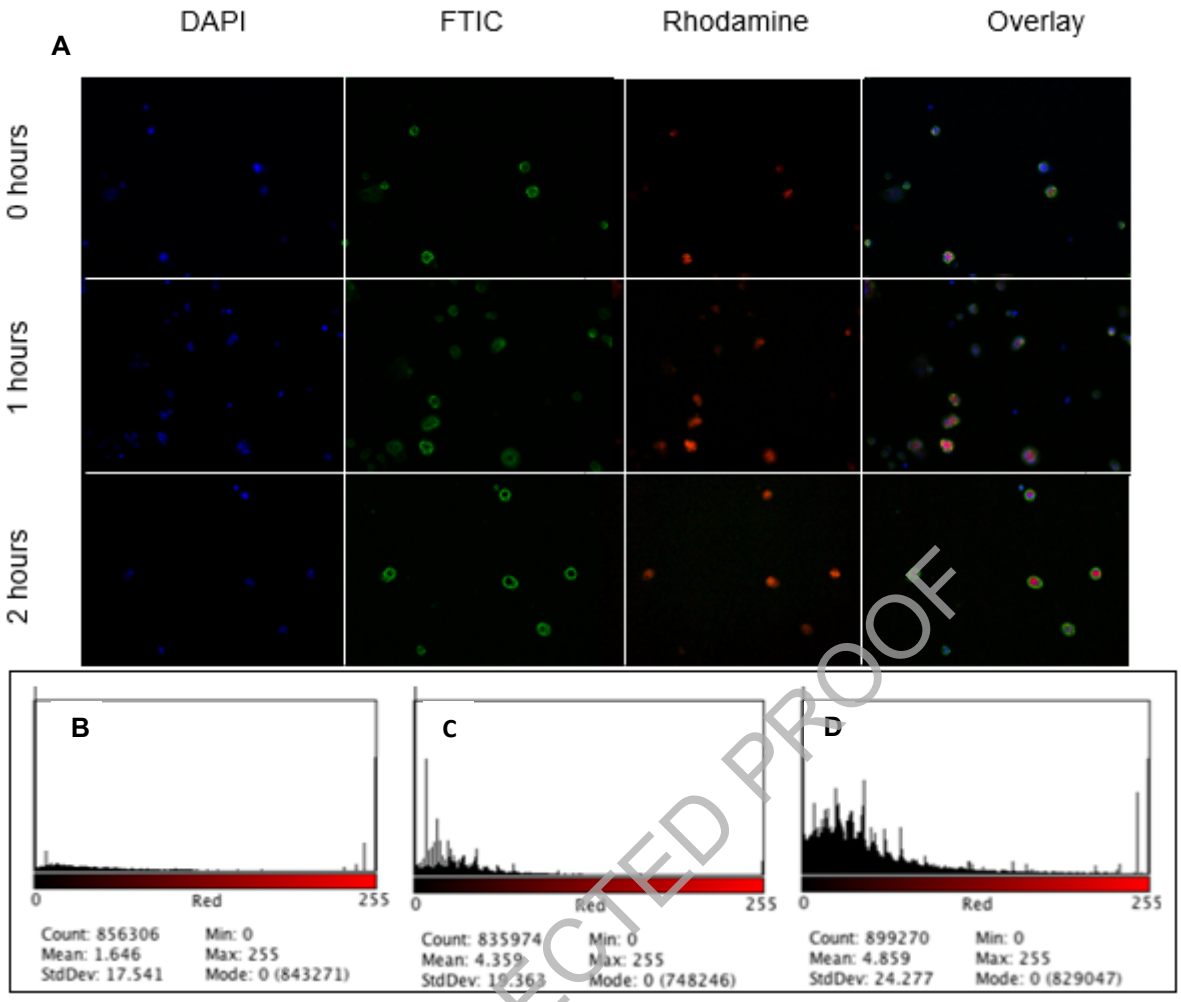

UNCORRECTED PROOF

Figure 5. Rhodamine incorporated Tam-β-CD-HA-Chi-Au nanocomposite uptake by Caco-2 cells. Caco-2 cells were analysed by fluorescence microscopy after 0 hours, 1 hours and 2 h of incubation with Tam-β-CD-HA-Chi-Au nanocomposite (A). The red-light intensity due to rhodamine incorporated Tam-β-CD-HA-Chi-Au nanocomposite represents the cellular uptake of the developed formulation at 0 h (B), 1 h (C) and 2 h (D).

Time	0 hour (h)	1 hour (h)	2 hours (h)
Intake of rhodamine incorporated Tam-β-CD-HA-Chi-Au nanocomposite	856306±17.541	835975±19.363	899272±24.277

Table 3. The intake of rhodamine incorporated Tam-β-CD-HA-Chi-Au nanocomposite deviation for 0 hour, 1 hour, and 2 hours is shown in the figure 5.

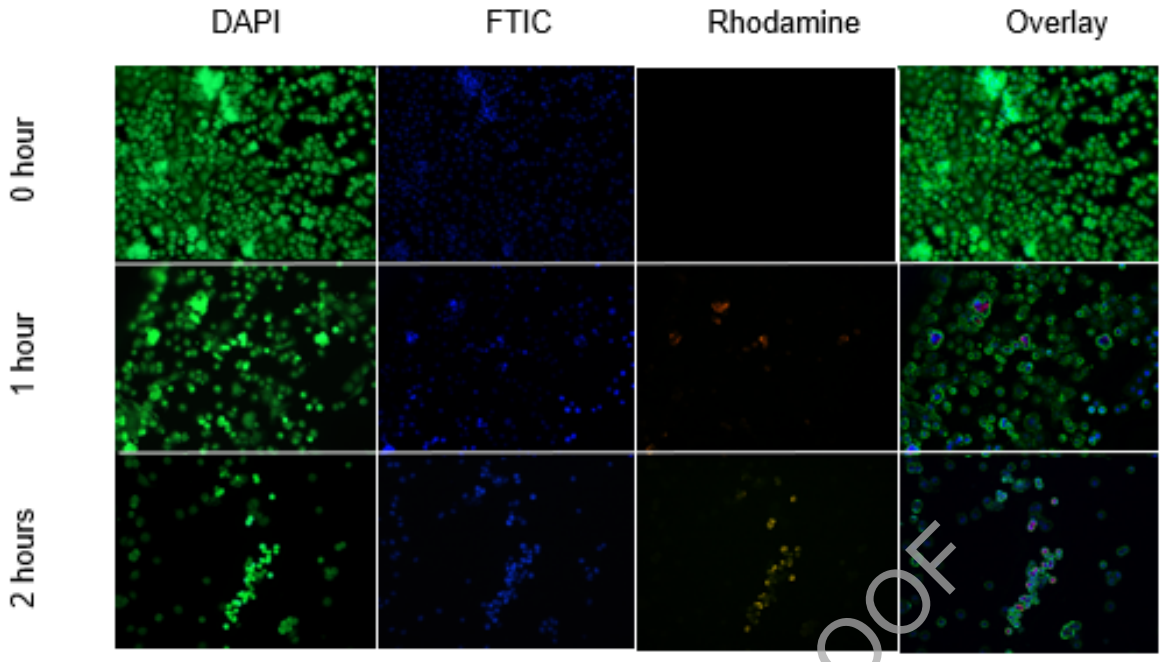

UNCORRECTED PROOF

Cytotoxicity of Tam-β-CD-HA-Chi-Au Nanocomposite on Caco-2 Cells and MCF-7

In this study, the Caco-2 and MCF-7 cells lines were used to investigate the cytotoxicity of Tam-β-CD-HA-Chi-Au nanocomposite on cancer cells, and the cellular impedance of the cells were monitored by a RTCA DP instrument. Figure 8A presents the dose-dependent cytotoxicity of Tam-β-CD-HA-Chi-Au nanocomposite on Caco-2 cell line. The Tam-β-CD-

Figure 6. Rhodamine incorporated Tam-β-CD-HA-Chi-Au nanocomposite uptake by MCF-7 cells were analysed by fluorescence microscopy after 0 h, 1 h and 2 h of incubation with Tam-β-CD-HA-Chi-Au nanocomposite). The red-light intensity due to rhodamine incorporated Tam-β-CD-HA-Chi-Au nanocomposite represents the cellular uptake of the developed formulation at 0 h, 1 h and 2 h.

HA-Chi-Au nanocomposite significantly improved the cytotoxic activity of Tam since the half maximal inhibitory concentration (IC_{50}) value of Tam was decreased from 8.55 µM to 5.32 µM after 48 hours of incubation time (p-value < 0.00001). Since intestinal epithelium of small and large intestine was normally surrounded by goblet cells which secrete a thick layer of mucus around them was postulated that the improvement in the cytotoxicity over time is due to the mucoadhesive and absorption enhancement properties of Chi. Similar study has shown that the keratinocyte growth (FGF7) FGF7:β-CD:everolimus complex has a significant cytotoxicity on Caco-2 cells and has improved the antiproliferative effect of everolimus. In other words, the FGF7:β-CD:everolimus complex succeeded in reducing the IC_{50} value of everolimus from 9.65 µM to 1.87 µM [39].On the other hand, no improvement in Tam cytotoxicity was observed when the nanocomposite was tested on MCF-7 cell line as the IC_{50} value of Tam was 6.48 µM which is lower than nanocomposite 68.6 µM after 48 hours of incubation time. It is mainly due to the lack of mucus lining around MCF-7 cells which prevents the adhesion of the nanocomposite to the cell surface and reduces the cellular uptake and consequently affect the cytotoxicity of Tam (Figure 8B).

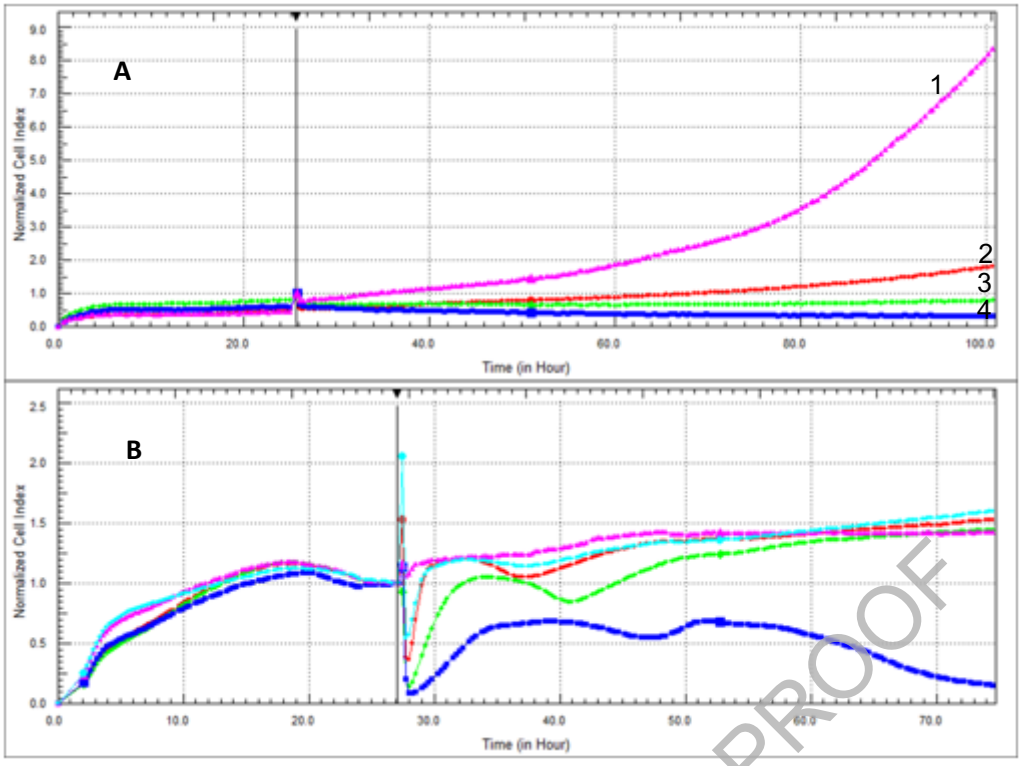

Figure 7. Cytotoxicity of Tam-β-CD-HA-Chi-Au nanocomposite on Caco-2 cells is shown by the RTCA DP instrument(8A). Cells were seeded and incubated with DMEM media(1A), 23.69 µM of Tam-β-CD-HA-Chi-Au nanocomposite(2A), 35.62 µM of Tam-β-CD-HA-Chi-Au nanocomposite (3A), 47.55 µM of Tam-β-CD-HA-Chi-Au nanocomposite (4A). Cytotoxicity of Tam-β-CD-HA-Chi-Au nanocomposite on MCF-7 cells is shown by the RTCA DP instrument(8B). Cells were seeded incubated with DMEM media (Pink), 2.15 µg of Tam-β-CD-HA-Chi-Au nanocomposite (Red), 3.23 µg of Tam-β-CD-HA-Chi-Au nanocomposite (Green), 4.31 µg of Tam-β-CD-HA-Chi-Au nanocomposite (Dark blue), Cells were seeded incubated with DMSO (Light blue).

UNCORRECTED PROOF

CONCLUSION

The Tam-β-CD-HA-Chi-Au nanocomposite was prepared successfully. These modified nanocomposites exhibited an average size of 82.02 nm with -23.6 mV zeta potential , Au occupied a central position, and a layer of polymers was surrounding the Au NPs which indicates a successful formulation of Au NPs, and a layer of Chi and the inclusion complex was deposited on the surface of NPs. Furthermore, Tam-β-CD-HA-Chi-Au nanocomposite (equivalent to 5.32 µM of tamoxifen citrate) significantly improved the cytotoxic activity and cellular uptake of Tam on Caco-2 cells. However, the developed formula showed more effect on Caco-2 than MCF-7. In conclusion, this research study showed that Tam-β-CD-HA-Chi-Au nanocomposite is a potential nanocarrier to deliver drug to cancer cells, due to its improved Tam activity on colorectal cancer cells.

Acknowledgment

This Project is supported by Pioneer Scientists Incentive Fund (PSIF) Under Centre of Excellence in Research, Value Innovation and Entrepreneurship (CERVIE), UCSI University, (Project Code: Proj-In-FPS-017) and Fundamental Research Grant Scheme (FRGS) (Reference code: FRGS/1/2021/SKK0/UCSI/02/5), Ministry of Higher Education (MOHE), Malaysia.

References

1. Li R, Xie Y. Nanodrug delivery systems for targeting the endogenous tumor microenvironment and simultaneously overcoming multidrug resistance properties. Journal of Controlled Release. 2017;251:49-67.
2. Bromma K, Chithrani DB. Advances in Gold Nanoparticle-Based Combined Cancer Therapy. Nanomaterials. 2020;10(9):1671.
3. Siegel RL, Miller KD, Goding Sauer A, Fedewa SA, Butterly LF, Anderson JC, et al. Colorectal cancer statistics, 2020. CA: a cancer journal for clinicians. 2020.
4. Zhao Y, Hu X, Zuo X, Wang M. Chemopreventive effects of some popular phytochemicals on human colon cancer: A review. Food & function. 2018;9(9):4548-68.
5. Howell A, Dowsett M. Recent advances in endocrine therapy of breast cancer. BMJ. 1997;315(7112):863-6.
6. Maeda H, Nakamura H, Fang J. The EPR effect for macromolecular drug delivery to solid tumors: Improvement of tumor uptake, lowering of systemic toxicity, and distinct tumor imaging in vivo. Advanced drug delivery reviews. 2013;65(1):71-9.
7. Bertrand N, Wu J, Xu X, Kamaly N, Farokhzad OC. Cancer nanotechnology: the impact of passive and active targeting in the era of modern cancer biology. Advanced drug delivery reviews. 2014;66:2-25.
8. Nazir S, Hussain T, Ayub A, Rashid U, MacRobert AJ. Nanomaterials in combating cancer: therapeutic applications and developments. Nanomedicine: Nanotechnology, Biology and Medicine. 2014;10(1):19-34.
9. Barenholz YC. Doxil®—the first FDA-approved nano-drug: lessons learned. Journal of controlled release. 2012;160(2):117-34.
10. Reynolds C, Barrera D, Jotte R, Spira AI, Weissman C, Boehm KA, et al. Phase II trial of nanoparticle albumin-bound paclitaxel, carboplatin, and bevacizumab in first-line patients with advanced nonsquamous non-small cell lung cancer. Journal of Thoracic Oncology. 2009;4(12):1537-43.
11. A Phase III Study of NK105 in Patients With Breast Cancer: US National Library of Medicine. Available from: https://clinicaltrials.gov/ct2/show/NCT01644890?term.
12. Silva JM, Videira M, Gaspar R, Préat V, Florindo HF. Immune system targeting by biodegradable nanoparticles for cancer vaccines. Journal of Controlled Release. 2013;168(2):179-99.
13. Shi J, Kantoff PW, Wooster R, Farokhzad OC. Cancer nanomedicine: progress, challenges and opportunities. Nature Reviews Cancer. 2017;17(1):20.
14. Thakor A, Jokerst J, Zavaleta C, Massoud T, Gambhir S. Gold nanoparticles: a revival in precious metal administration to patients. Nano letters. 2011;11(10):4029-36.
15. Koushik O, Rao Y, Kumar P, Karthikeyan R. Nano drug delivery systems to overcome cancer drug resistance—a review. J Nanomed Nanotechnol. 2016;7(378):2.
16. Li W, Zhang H, Assaraf YG, Zhao K, Xu X, Xie J, et al. Overcoming ABC transporter-mediated multidrug resistance: Molecular mechanisms and novel therapeutic drug strategies. Drug Resistance Updates. 2016;27:14-29.
17. Haley B, Frenkel E, editors. Nanoparticles for drug delivery in cancer treatment. Urologic Oncology: Seminars and original investigations; 2008: Elsevier.
18. Creixell M, Peppas NA. Co-delivery of siRNA and therapeutic agents using nanocarriers to overcome cancer resistance. Nano today. 2012;7(4):367-79.
19. Akpan E, Gbenebor O, Adeosun S, Cletus O. Solubility, degree of acetylation, and distribution of acetyl groups in chitosan. Handbook of Chitin and Chitosan: Elsevier; 2020. p. 131-64.
20. Yu S, Xu X, Feng J, Liu M, Hu K. Chitosan and chitosan coating nanoparticles for the treatment of brain disease. International journal of pharmaceutics. 2019;560:282-93.

UNCORRECTED PROOF

21. Shariatinia Z. Pharmaceutical applications of chitosan. Advances in Colloid and Interface Science. 2019;263:131-94.
22. Priotti J, Baglioni MV, García A, Rico MJ, Leonardi D, Lamas MC, et al. Repositioning of anti-parasitic drugs in cyclodextrin inclusion complexes for treatment of triple-negative breast cancer. AAPS PharmSciTech. 2018;19(8):3734-41.
23. SreeHarsha N, Hiremath JG, Chilukuri S, Aitha RK, Al-Dhubiab BE, Venugopala KN, et al. An approach to enhance dissolution rate of tamoxifen citrate. BioMed research international. 2019;2019.
24. Vijayakumar A, Baskaran R, Jang YS, Oh SH, Yoo BK. Quercetin-loaded solid lipid nanoparticle dispersion with improved physicochemical properties and cellular uptake. AAPS PharmSciTech. 2017;18(3):875-83.
25. Zhang Y, Li Z, Zhang K, Yang G, Wang Z, Zhao J, et al. Ethyl oleate-containing nanostructured lipid carriers improve oral bioavailability of trans-ferulic acid ascompared with conventional solid lipid nanoparticles. International journal of pharmaceutics. 2016;511(1):57-64.
26. Subedi RK, Kang KW, Choi H-K. Preparation and characterization of solid lipid nanoparticles loaded with doxorubicin. European journal of pharmaceutical sciences. 2009;37(3-4):508-13.
27. Santana DPd, Braga RMC, Strattmman R, Albuquerque MM, Bedor DCG, Leal LB, et al. Reversed phase HPLC determination of tamoxifen in dog plasma and its pharmaco-kinetics after a single oral dose administration. Quimica Nova. 2008;31(1):47-52.
28. Spötl L, Sarti A, Dierich MP, Möst J. Cell membrane labeling with fluorescent dyes for the demonstration of cytokine-induced fusion between monocytes and tumor cells. Cytometry: The Journal of the International Society for Analytical Cytology. 1995;21(2):160-9.
29. Turkevich J, Stevenson PC, Hillier J. A study of the nucleation and growth processes in the synthesis of colloidal gold. Discussions of the Faraday Society. 1951;11:55-75.
30. Nivethaa E, Dhanavel S, Narayanan V, Vasu CA, Stephen A. An in vitro cytotoxicity study of 5-fluorouracil encapsulated chitosan/gold nanocomposites towards MCF-7 cells. RSC Advances. 2015;5(2):1024-32.
31. Mattheolabakis G, Milane L, Singh A, Amiji MM. Hyaluronic acid targeting of CD44 for cancer therapy: from receptor biology to nanomedicine. Journal of drug targeting. 2015;23(7-8):605-18.
32. Prabhakar U, Maeda H, Jain RK, Sevick-Muraca EM, Zamboni W, Farokhzad OC, et al. Challenges and key considerations of the enhanced permeability and retention effect for nanomedicine drug delivery in oncology. AACR; 2013.
33. Rampino A, Borgogna M, Blasi P, Bellich B, Cesàro A. Chitosan nanoparticles: preparation, size evolution and stability. International journal of pharmaceutics. 2013;455(1-2):219-28.
34. Abdulkin P, Precht TL, Knappett BR, Skelton HE, Jefferson DA, Wheatley AE. Systematic control of size and morphology in the synthesis of gold nanoparticles. Particle & Particle Systems Characterization. 2014;31(5):571-9.
35. Setyawati MI, Tay CY, Bay BH, Leong DT. Gold nanoparticles induced endothelial leakiness depends on particle size and endothelial cell origin. ACS nano. 2017;11(5):5020-30.
36. Regiel-Futyra A, Kus-Liśkiewicz M, Sebastian V, Irusta S, Arruebo M, Stochel Gy, et al. Development of noncytotoxic chitosan–gold nanocomposites as efficient antibacterial materials. ACS applied materials & interfaces. 2015;7(2):1087-99.
37. Kang JH, Ko YT. Lipid-coated gold nanocomposites for enhanced cancer therapy. International journal of nanomedicine. 2015;10(Spec Iss):33.

UNCORRECTED PROOF

38. Bindhu M, Umadevi M. Silver and gold nanoparticles for sensor and antibacterial applications. Spectrochimica Acta Part A: Molecular and Biomolecular Spectroscopy. 2014;128:37-45.
39. Maki MAA, Cheah S-C, Bayazeid O, Kumar PV. Cyclodextrin inclusion complex inhibits circulating galectin-3 and FGF-7 and affects the reproductive integrity and mobility of Caco-2 cells. Scientific reports. 2020;10(1):1-8.

UNCORRECTED PROOF